Thermodynamics of redox equilibrium in slags

Nobuo Sano[1)] and Fumitaka Tsukihashi[2)]

1) Professor emeritus, The University of Tokyo,
and Executive advisor, Nippon Steel Corporation
2) Professor, The University of Tokyo

Abstract : The transition metals are known to effects on the characteristics of slags and refining capacities of slags. On the other hand, the redox equilibria of transition metal ions have been reported for the measure of slag basicity. The effects of the slag composition, oxygen partial pressure and temperature on the redox equilibria of various elements, such as iron, manganese, copper and titanium, etc., in slags were summarized. The relationship between the redox equilibria and other basicity indexes, such as various capacities, activity of calcium oxide and theoretical optical basicity are discussed.

1. Introduction

Slags are formed during the metal refining processes. The industrial slags encountered in metallurgical processes contain various elements and their redox reactions affect the characteristics of slags and refining capacities of slags. Therefore, it is needed to investigate the thermodynamics of redox equilibrium for slags in metal refining processes. Because highly basic slags are increasingly required for refining, a well defined measure of slag basicity is needed. However, since the basicity defined by the activity of oxide ion cannot be measured in principle, alternative way of description of basicity is still sought.

In this paper, the thermodynamics of redox equilibria of various elements in metallurgical slags are summarized and the application of redox equilibria for the measure of basicity is discussed.

2. Redox equilibrium of various ions in slags

2.1. Iron

The stable forms of iron in slags are Fe^{2+} and Fe^{3+} and in steelmaking or copper smelting slags the two species always coexist. As shown in Fig. 1[1)] , the Fe^{3+}/ Fe^{2+} ratio increases as CaO content of the CaO-FeO-Fe_2O_3 system increases at a constant partial pressure of oxygen. This is explained by postulating the presence of anions of $FeO_n^{(2n-3)-}$ such as FeO_2^- as in Eq. (1). However, in acid slags such as iron silicates in copper smelting, the cation Fe^{3+} would be predominant as shown by Eq. (2). The exchange reaction between Fe^{3+} and FeO_2^- is expressed as Eq. (3) and in basic slags FeO_2^- is predominant rather than Fe^{3+}.

$$(Fe^{2+}) + \frac{1}{4}O_2(g) + \frac{3}{2}(O^{2-}) = (FeO_2^-) \qquad (1)$$

$$(Fe^{2+}) + \frac{1}{4}O_2(g) = (Fe^{3+}) + \frac{1}{2}(O^{2-}) \qquad (2)$$

$$(Fe^{3+}) + 2(O^{2-}) = (FeO_2^-) \qquad (3)$$

The activity of FeO as well as of MnO is greatly enhanced by the presence of halide.

Figure 2[2] shows the activity of FeO against FeO content for the FeO-CaF_2 system. In the CaO-SiO_2-FeO system, the activity of FeO has a maximum at X_{CaO}/X_{SiO2} = 2 at a constant FeO content. This may be explained by a fact that the orthosilicate composition is most stable in the CaO-SiO_2 system.

2.2. Manganese

The stable species of manganese in slags is Mn^{2+} in most cases. Even in air, Mn^{3+} is a minor species, as shown in Fig. 3[3] for the Mn^{3+}/Mn^{2+} equilibrium of CaO-Mn_tO-SiO_2 melts. The ratio increases with increasing slag basicity. Accordingly, the equilibrium may be described by Eq. (4). In the steelmaking process, the manganese equilibrium between slag and molten steel is shown as Eq. (5). Since MnO is a basic oxide, the yield of manganese is improved by using basic slags according to Eq. (5) and Fig. 4[4].

$$(Mn^{2+}) + \frac{1}{4}O_2(g) + \frac{3}{2}(O^{2-}) = (MnO_2^-) \qquad (4)$$

$$[Mn]_{\text{in metal}} + \frac{1}{2}O_2(g) = (Mn^{2+}) + (O^{2-}) \qquad (5)$$

2.3. Chromium

Chromium is present as Cr^{2+}, Cr^{3+}, or Cr^{6+} in slags depending on the prevailing oxygen pressure. Figure 5[5] shows that the activity coefficient of CrO increases with increasing $(X_{CaO}+X_{AlO1.5})/X_{SiO2}$, indicating that CrO is a weakly basic oxide in the CaO-$AlO_{1.5}$-SiO_2 system. Cr^{6+} is stable as CrO_4^{2-}, so that as Fig. 6[6] shows for the MgO-SiO_2-CaO system at 1873K in air, Cr^{6+}/Cr^{3+} increases with increasing slag basicity as indicated by Eq. (6).

$$(Cr^{3+}) + \frac{5}{2}O_2(g) + \frac{3}{4}(O^{2-}) = (CrO_4^{2-}) \qquad (6)$$

The effect of X_{CaO}/X_{SiO2} on the Cr^{3+}/Cr^{2+} for the CaO-SiO_2-CrO_x system at 1873K with P_{O2} = 7.04x10^{-6} Pa is presented in Figure 7[7]. The Cr^{3+}/Cr^{2+} ratio significantly increases with increasing slag basicity.

2.4. Titanium

The stable species of titanium in most slags are Ti^{3+} and Ti^{4+}. The latter in particular behaves as an amphoteric oxide as shown in Fig. 8[8], which shows the activity of TiO_2 for the CaO-Al_2O_3-SiO_2 system. It has a maximum with changing the ratio CaO/SiO_2 at constant Al_2O_3. Figure 9[9] shows the relationship between $Ti^{3+}/(Ti^{3+}+Ti^{4+})$ and $SiO_2/(SiO_2+MnO)$ for the MnO-SiO_2-TiO_x system at 1573K with very low oxygen partial pressure. The content of Ti^{3+} increases with decreasing the slag basicity. Therefore, Ti^{4+} ion may exist in the form of complex ion such as TiO_3^{2-} according to Eq. (7).

$$(Ti^{3+}) + \frac{1}{4}O_2(g) + \frac{5}{2}(O^{2-}) = (TiO_3^{2-}) \qquad (7)$$

The relationship between Ti^{4+}/Ti^{3+} ratio in $2MnO \cdot TiO_x$ and oxygen partial pressure is shown in Fig. 10[9]. The ratio increases with increasing the partial pressure of oxygen. However, the slope of line in Fig. 10, 0.104, does not agree well with the expected one, 0.25, according to Eq. (7). This is probably because the ratio of activity coefficients of Ti^{3+} and Ti^{4+} varies with changing composition.

2.5. Niobium, vanadium and antimony

Niobium, vanadium and antimony exist in basic slags mostly as anions. The valence of vanadium changes from V^{2+} to V^{5+}, antimony does from Sb^{2+} to Sb^{4+}, and the valence of niobium is nearly Nb^{5+} in the Na_2O-SiO_2 system at 1473K at the oxygen partial pressure determined by the C-CO equilibrium, as shown in Fig. 11[10].

2.6. Copper

Figures 12, and 13[11] show the relationship between Cu^{2+}/Cu^{+} ratio and slag composition for the $NaO_{0.5}$-SiO_2 and $NaO_{0.5}$-NaF-SiO_2 systems at 1373K, and for the CaO -SiO_2 system at 1823K in air. The Cu^{2+}/Cu^{+} ratio decreases with increasing the basic composition of slags. The dependence of the Cu^{2+}/Cu^{+} ratio on the partial pressure of oxygen for the 17mol%$NaO_{0.5}$ -38mol%CaO -SiO_2 system at 1673K is shown in Fig. 14[11]. The slope of the line in Fig. 15, 0.32, is close to 0.25, which is expected by Eq. (8).

$$(Cu^{+}) + \frac{1}{4}O_2(g) = (Cu^{2+}) + \frac{1}{2}(O^{2-}) \qquad (8)$$

2.7. Phosphorus

Phosphorus is stable in slags either as PO_4^{3-} or P^{3-}, depending upon the prevailing oxygen partial pressure. Figure 15[12] shows the variation of phosphorus content of a CaO-Al_2O_3 melt with oxygen partial pressure under a constant phosphorus pressure at 1823K. Equations (9) and (10) is the reaction of phosphorus vapor dissolved into slags as PO_4^{3-} or P^{3-}. The slopes of two lines in Fig. 15 are close to expected values, 5/4 for higher oxygen partial pressure and –3/4 for lower oxygen partial pressure.

$$\frac{1}{2}P_2(g) + \frac{5}{4}O_2(g) + \frac{3}{2}(O^{2-}) = (PO_4^{3-}) \qquad (9)$$

$$\frac{1}{2}P_2(g) + \frac{3}{2}(O^{2-}) = (P^{3-}) + \frac{3}{4}O_2(g) \qquad (10)$$

2.8. Sulfur

Similar to the case of phosphorus, sulfur contents of two oxide melts under a constant partial pressure of SO_2 are shown in Fig. 16[13]. Sulfate is predominant species at oxygen partial pressures higher than that determined by $CaSO_4$-CaS equilibrium reaction expressed by Eq. (11) and sulfide is predominant at lower oxygen partial pressures. These reactions are shown by Eqs. (12) and (13). Since the oxygen partial pressure in steelmaking is far below the critical oxygen partial pressure, the sulfide is stable in slags and desulfurization reaction is written as Eq. (14).

$$CaS(s) + 2O_2(g) = CaSO_4(s) \qquad (11)$$

$$\frac{1}{2}O_2(g) + SO_2(g) + (O^{2-}) = (SO_4^{2-}) \qquad (12)$$

$$SO_2(g) + (O^{2-}) = (S^{2-}) + \frac{3}{2}O_2(g) \qquad (13)$$

$$[S]_{\text{in metal}} + (O^{2-}) = (S^{2-}) + \frac{1}{2}O_2(g) \qquad (14)$$

2.9. Carbon

Carbon is known to dissolve in slags as carbonate ion at higher oxygen partial pressures and as carbide ion at lower oxygen partial pressures according to reactions (15) and (16). The reactions of carbide, $M_{0.5}C$, oxide, MO, and carbonate, MCO_3 (M: Ca, Ba) are expressed by Eqs. (17) and (18). Figures 17 and 18[14] show the effect of oxygen partial pressure on the carbon content of slag for the 80mass%BaO-MnO system at 1573K and for the $CaO_{satd.}$-B_2O_3 system at 1733K. Below and beyond a critical partial pressure of oxygen, log P_{O2}(atm)=-14.6 for the BaO-MnO system and P_{O2}(atm)=-11.7 for the $CaO_{satd.}$-B_2O_3 system, respectively, carbide and carbonate are predominant species as expected from Eqs. (17) and (18).

$$C(s) + O_2(g) + (O^{2-}) = (CO_3^{2-}) \qquad (15)$$

$$2C(s) + (O^{2-}) = (C_2^{2-}) + \frac{1}{2}O_2(g) \qquad (16)$$

$$\frac{1}{2}(MO) + CO(g) = (M_{0.5}C) + \frac{3}{4}O_2(g) \qquad (17)$$

$$(MO) + CO(g) + \frac{1}{2}O_2(g) = (MCO_3) \qquad (18)$$

3. Measure of basicity

The basicity of slags is the most important characteristics for refining of metals. Although the basicity is theoretically defined by the activity of an oxide ion, it cannot be determined experimentally. Therefore, a number of measures for slag basicity index have been practically used and various measures have been proposed such as redox equilibrium of transition metal ions, solubility of CO_2 gas in slag, and optical basicity.

3.1. Redox equilibrium of copper in slag

The relationships between the Cu^{2+}/Cu^{+} ratio and carbonate capacity and the optical basicity are shown in Figs. 19 and 20[11] for various slag systems. The $\log(Cu^{2+}/Cu^{+})$ has linear relationship with logarithm of sulfide capacity and optical basicity.

3.2. Platinum solubility of slags

The reaction of platinum dissolution into basic slags can be written as Eq. (19). Figures 21, 22 and 23[15,16] show the solubility of platinum in various slag systems in air at 1873K. The solubilities increase with increasing the contents of basic oxide in slag. The correlations among the solubility of platinum, various capacities, activity of basic oxide, and theoretical optical basicity are represented in Figs. 24, 25 and 26[15]. The solubility of platinum has a linear relationship with carbonate, phosphate and sulfide capacities, activity of basic oxides and theoretical optical basicity in logarithmic form. It is suggested that the solubility of platinum in slags may be a good indicator of basicity of highly basic slags.

$$Pt(s) + \frac{1}{2}O_2(g) + (O^{2-}) = (PtO_2^{2-}) \qquad (19)$$

4. Conclusions

Redox equilibria of various elements in slags are summarized and the description of the measure of basicity is discussed. Thermodynamic properties of redox equilibrium in slags must be further investigated for wider use in practice.

References

1) E.T.Turkdogan : Physicochemical Properties of Molten Slags and Glasses, The Metal Society, London, p.241.
2) M.W.Davies: Chemical Metallurgy of Iron and Steel, The Iron and Steel Institute, p.45.
3) Y.Tamura, S.Nakamura and N.Sano: Tetsu-toHagane, **73** (1987), pp.2214-2218.
4) E.T.Turkdogan : Physicochemical Properties of Molten Slags and Glasses, The Metal Society, London, p.281.
5) M.Maeda and N.Sano: Tetsu-toHagane, **68** (1982), pp.759-766.
6) K.Morita, T.Shibuya and N.Sano: Tetsu-toHagane, **74** (1988), pp.632-639.
7) K.Morita, M.Mori, M.Guo, T.Ikagawa and N.Sano: steel research, **70** (1999), pp.319-324.
8) K.Ito and N.Sano: Tetsu-toHagane, **67** (1981), pp.2131-2137.
9) H.Amitani, K.Morita and N.Sano: ISIJ International, **36** (1996), pp.S26-29.
10) F.Tsukihashi, A.Werme, A.Kasahara, M.Okada and N.Sano: Tetsu-toHagane, **71** (1985), pp.831-838.
11) S.Nakamura and N.Sano: Metall. Trans. B, **22B** (1991), pp.823-829.
12) H.Momokawa and N.Sano: Metall. Trans. B, **13B** (1982), pp.643-644.
13) H.E.McGannon(ed.) : The Making, Shaping and Treating of Steel, 8th edition, United States Steel, p.352.
14) M.Mori, K.Morita and N.Sano: Metall. Material Trans. B, **28B** (1997), pp.1257-1260.
15) S.Nakamura and N.Sano: Metall. Material Trans. B, **28B** (1997), pp.103-108.
16) S.Nakamura, K.Iwazawa, K.Morita and N.Sano: Metall. Material Trans. B, **29B** (1998), pp.411-414.

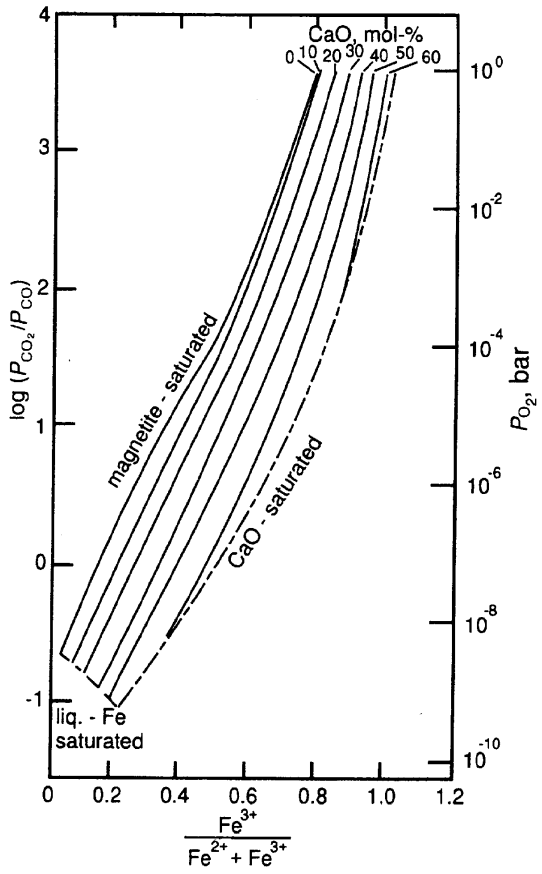

Fig. 1. State of oxidation of iron in CaO-FeO-Fe_2O_3 melts at 1823K.

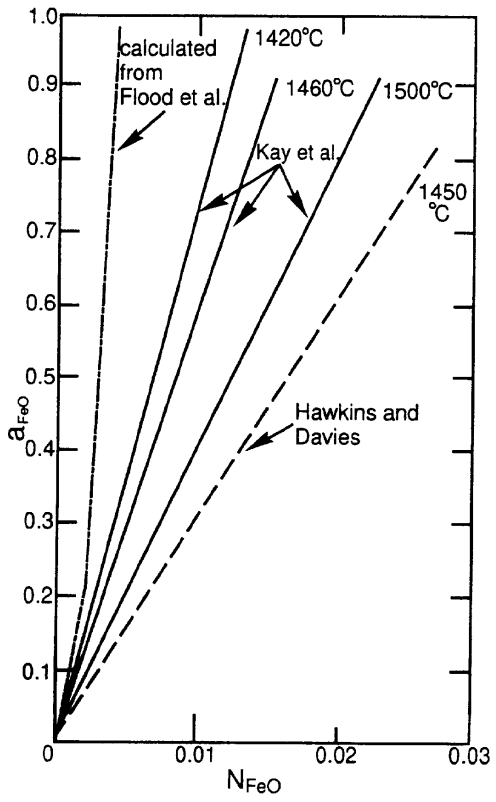

Fig. 2. Activity of FeO in the CaF_2-FeO system.

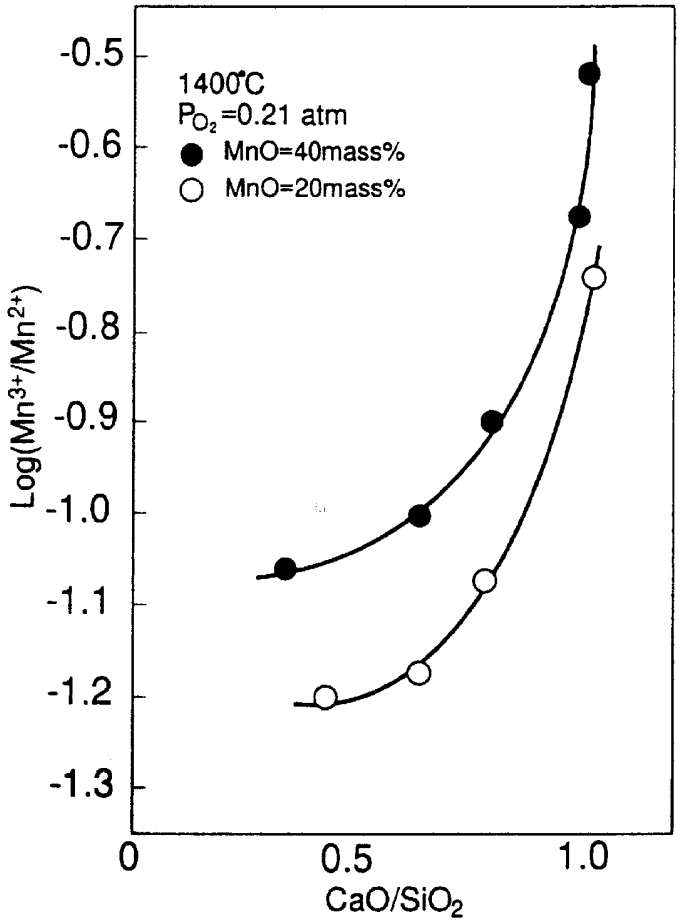

Fig. 3. $Log(\%Mn^{3+})/(\%Mn^{2+})$ for the $CaO\text{-}Mn_tO\text{-}SiO_2$ system as a function of CaO/SiO_2 in air at 1673K.

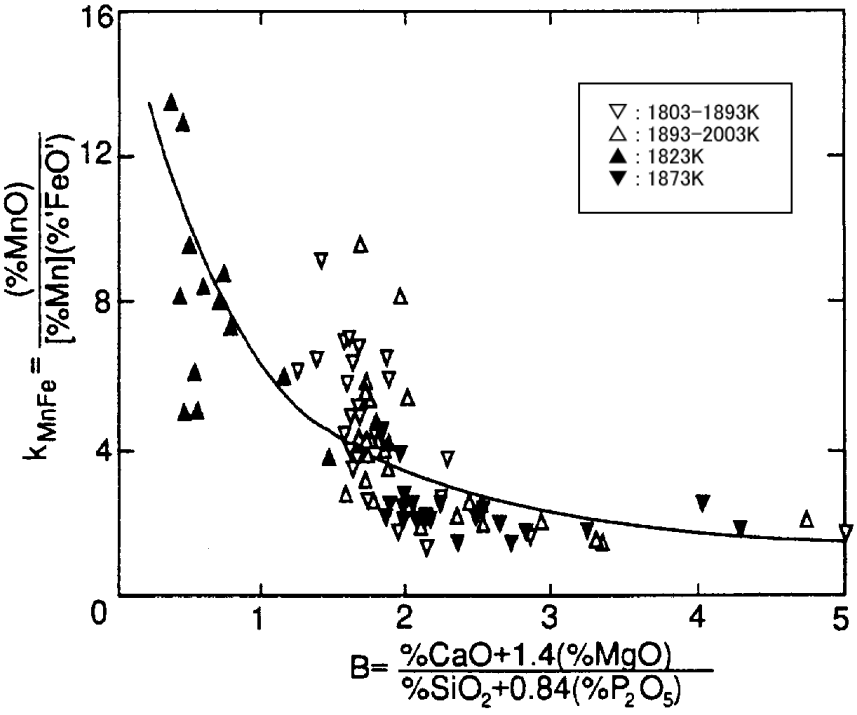

Fig. 4. Variation in the equilibrium relationship k_{MnFe} for manganese reaction with slag basisity.

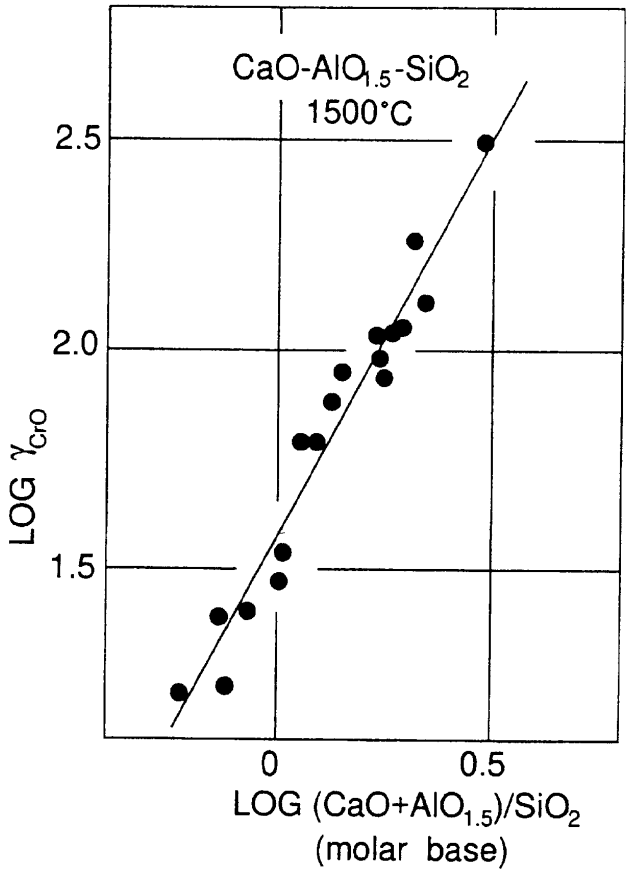

Fig. 5. Relationship between activity coefficient of CrO and molar ratio $(CaO+AlO_{1.5})/SiO_2$ for the $CaO\text{-}AlO_{1.5}\text{-}SiO_2$ system.

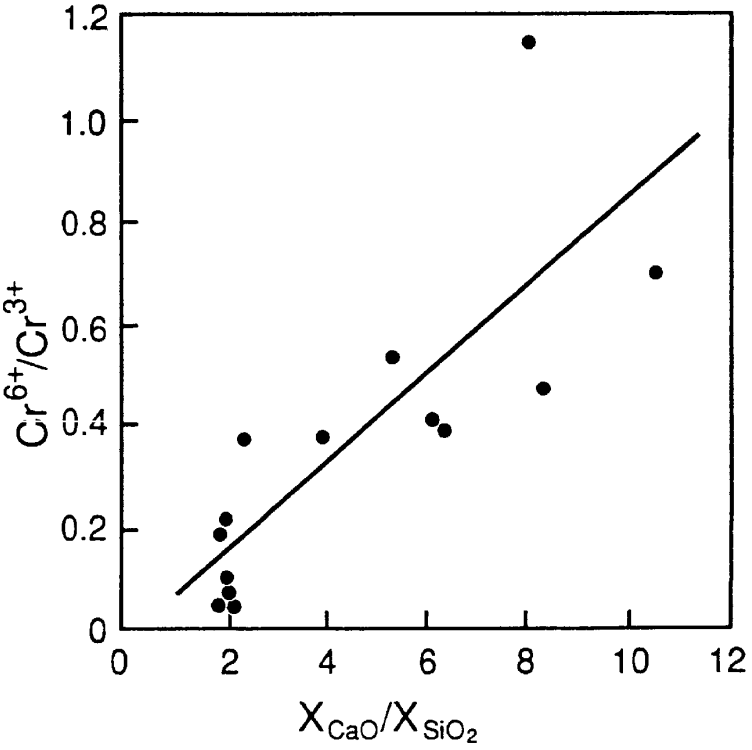

Fig. 6. Basicity dependence of the Cr^{6+}/Cr^{3+} ratio in $MgO\text{-}SiO_2\text{-}CaO\text{-}CrO_x$ melts at 1873K in air.

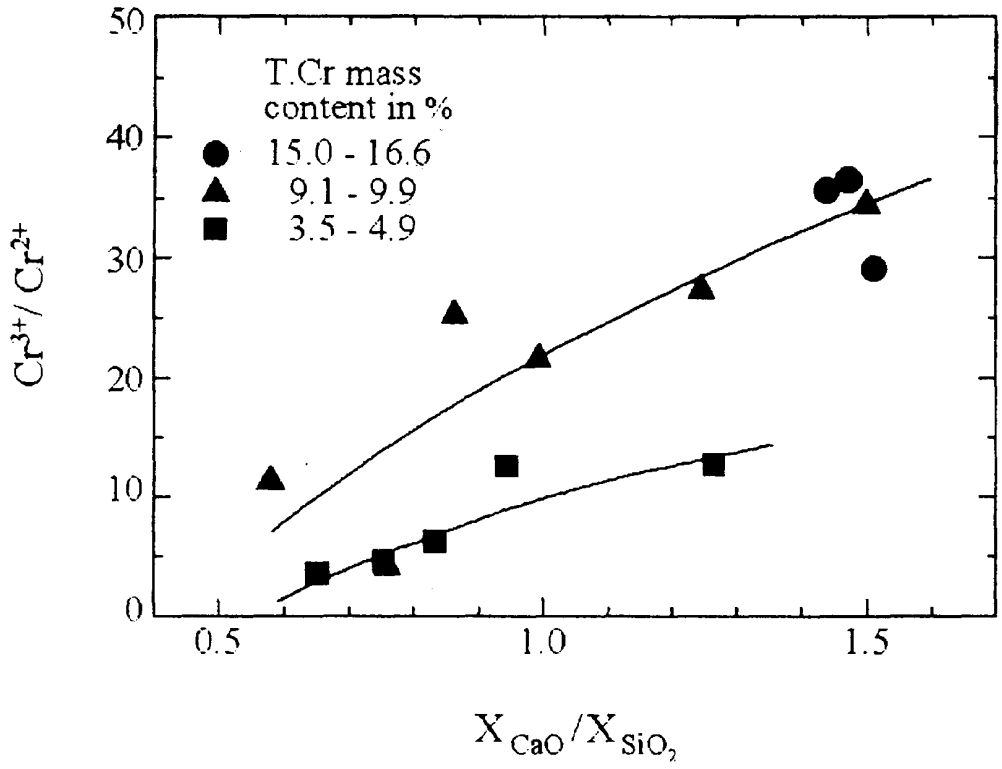

Fig. 7. Effect of X_{CaO}/X_{SiO2} on the Cr^{3+}/Cr^{2+} ratio for the CaO-SiO_2-CrO_x system at 1873K with P_{O2} = 7.04x10^{-6} Pa..

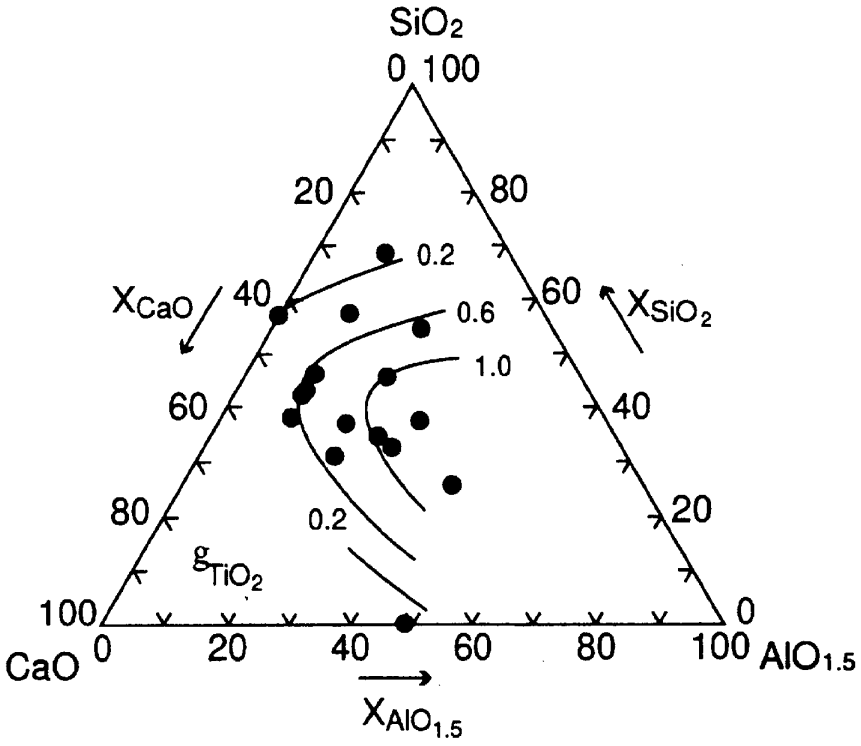

Fig. 8. Contours of activity coefficient for TiO_2 in the CaO-$AlO_{1.5}$-SiO_2 system at 1773K.

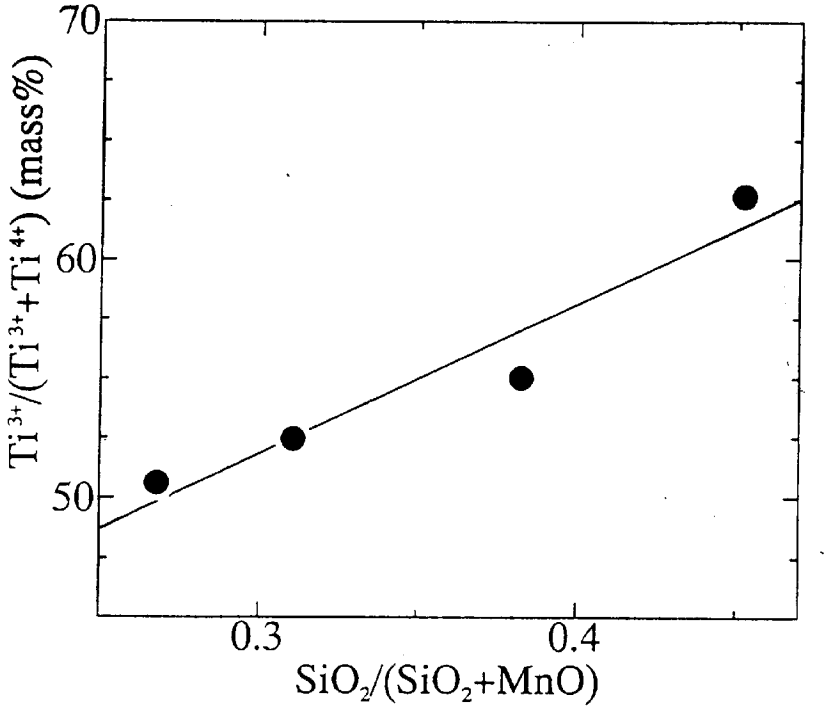

Fig. 9. Relationship between $Ti^{3+}/(Ti^{3+}+Ti^{4+})$ along the Ti_2O_3 liquidus and $SiO_2/(SiO_2+MnO)$.

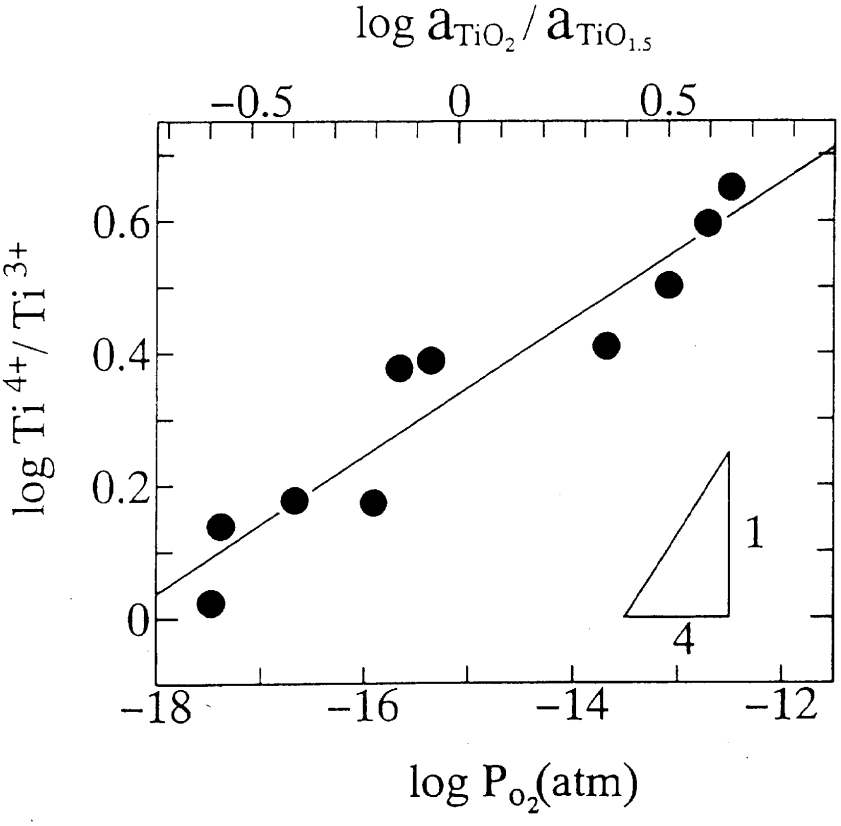

Fig. 10. Dependence of the Ti^{4+}/Ti^{3+} ratio in $2MnOTiO_x$ on oxygen partial pressure at 1573K.

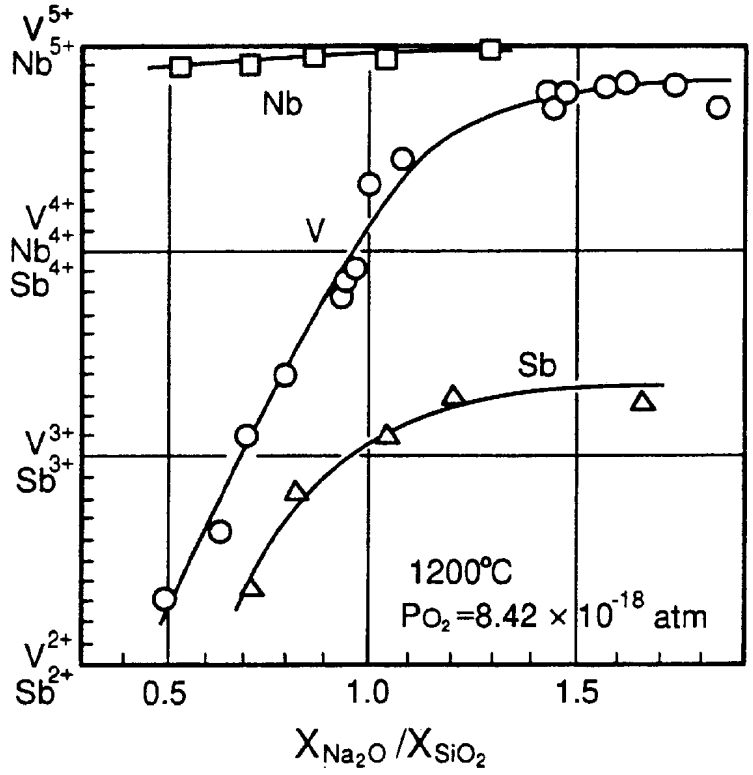

Fig. 11. Change in valences of vanadium, niobium, and antimony with the composition of the Na_2O-SiO_2 system at 1473K.

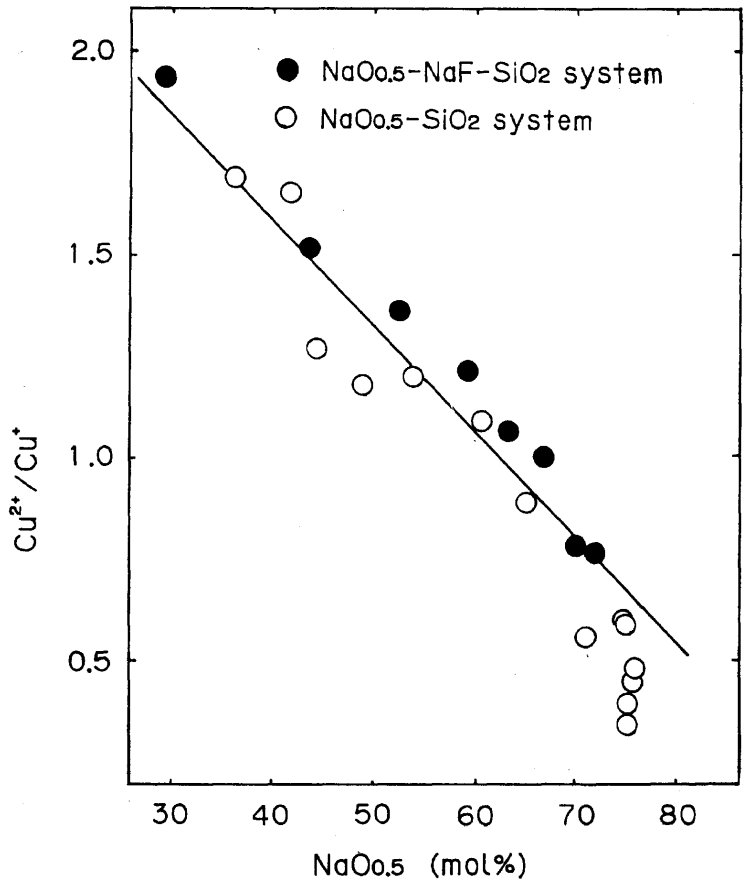

Fig. 12. Dependence of the Cu^{2+}/Cu^{+} ratio on $Na_{0.5}O$ for the $NaO_{0.5}$-SiO_2 and $NaO_{0.5}$-11mol %NaF-SiO_2 system in air at 1373K.

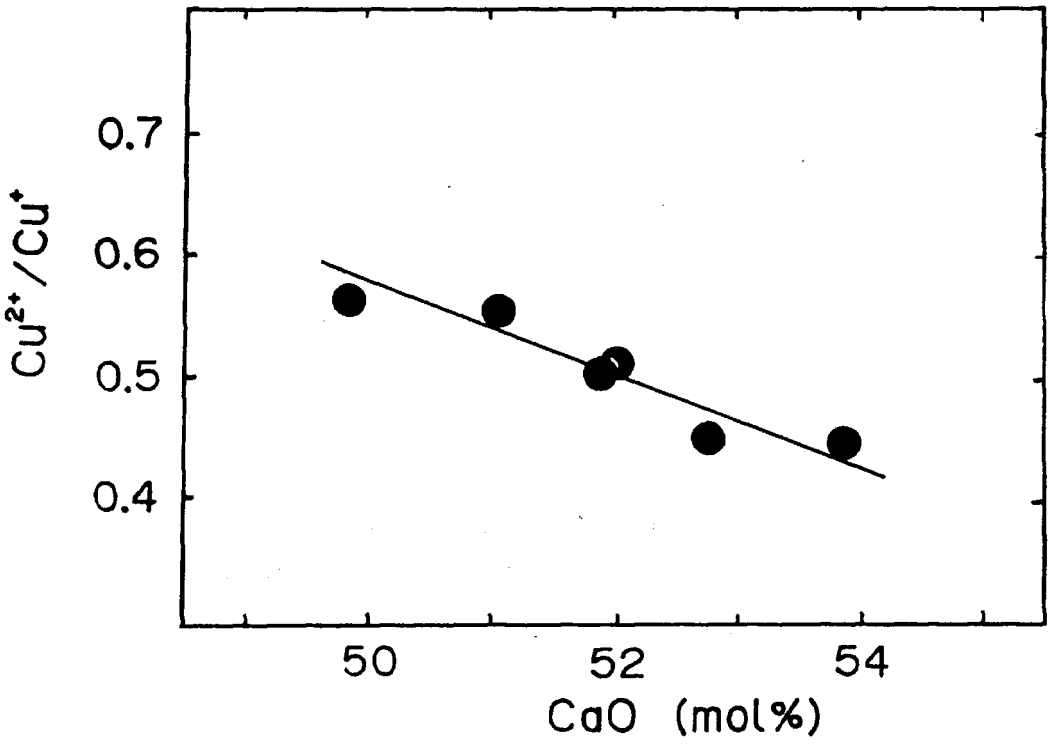

Fig. 13. Dependence of the Cu^{2+}/Cu^{+} ratio on CaO Content for the $CaO\text{-}SiO_2$ system in air at 1823K.

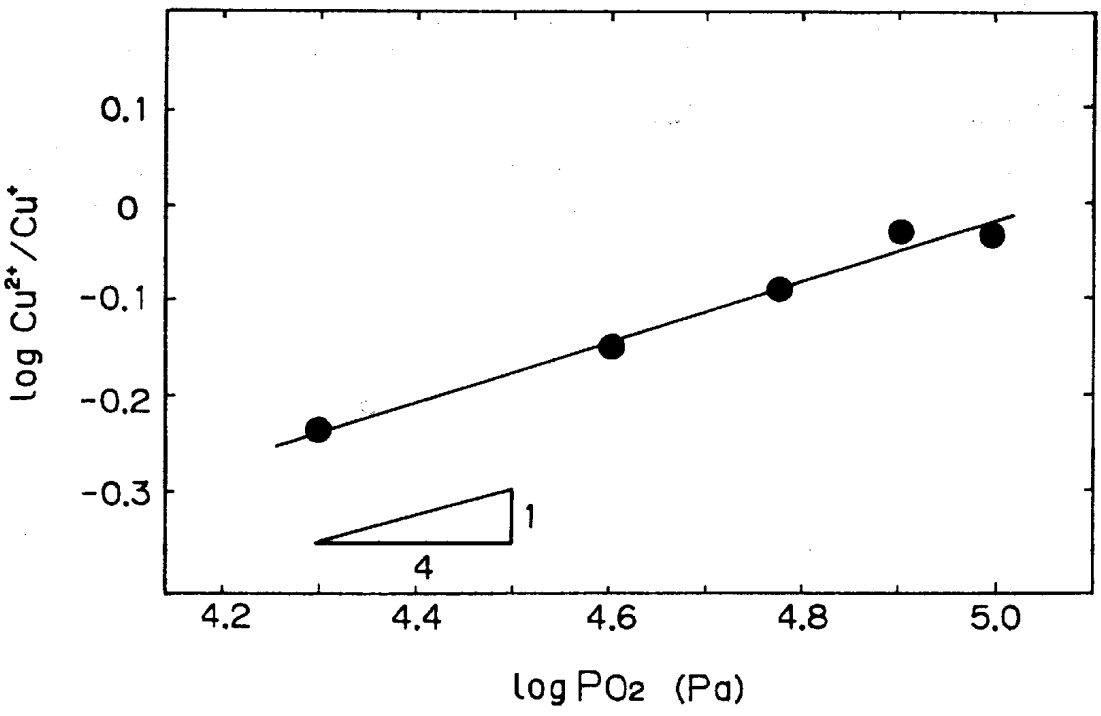

Fig. 14. Dependence of the Cu^{2+}/Cu^{+} ratio on partial pressure of oxygen for the $17mol\%NaO_{0.5}\text{-}38mol\%CaO\text{-}SiO_2$ system at 1673K.

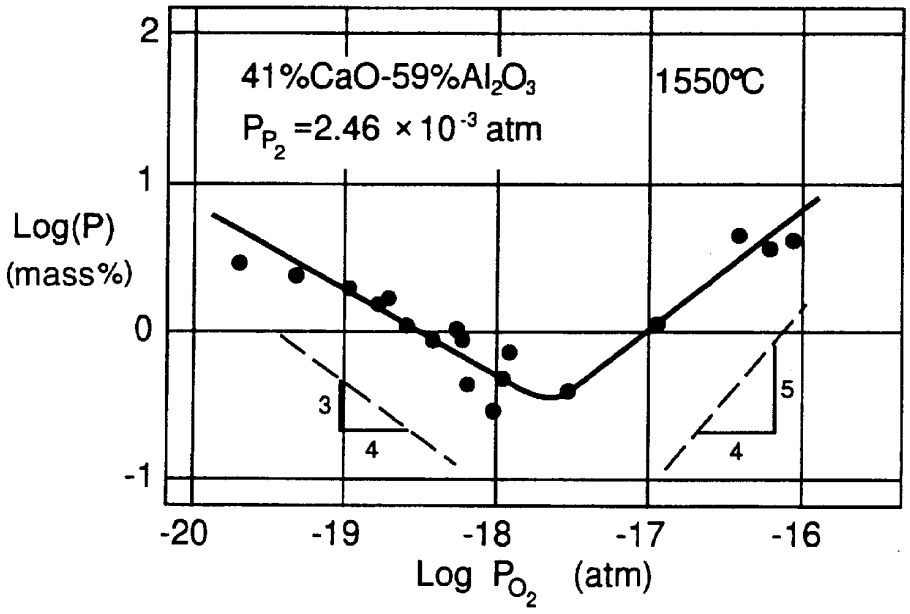

Fig. 15. Variation in phosphorus content of the $CaO\text{-}Al_2O_3$ melt with partial pressure of oxygen.

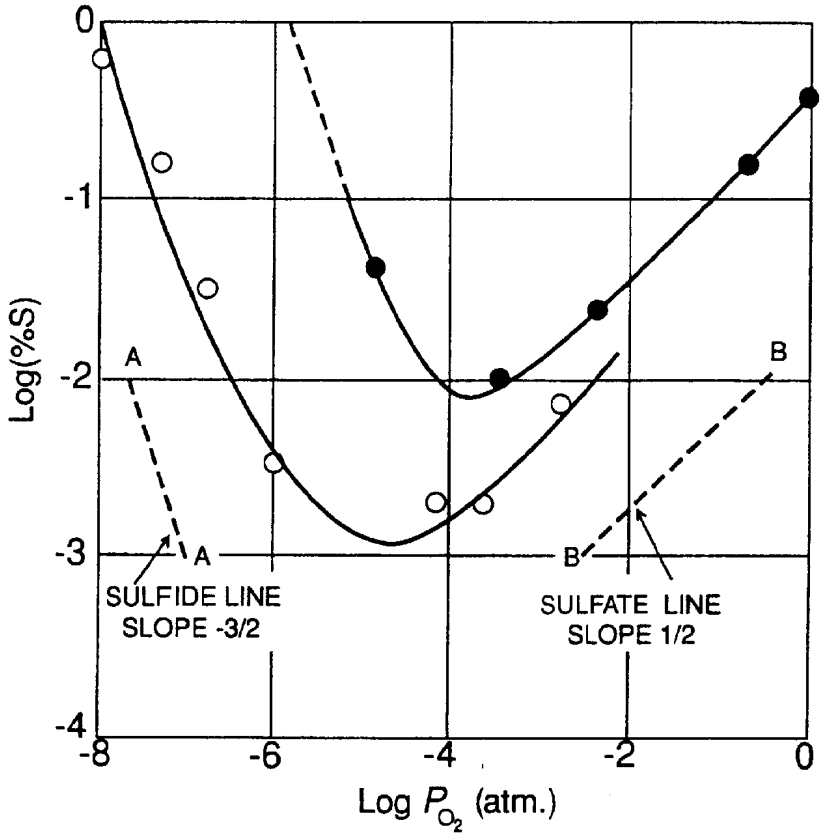

Fig. 16. Variation in sulfur content of oxide melts with partial pressure of oxygen. (Solid circles: calcium ferrite melts at 1893K and P_{SO2} 6-8%. Open circles: calcium-alumino-silicate melts at 1773K and P_{SO2} = 2%.)

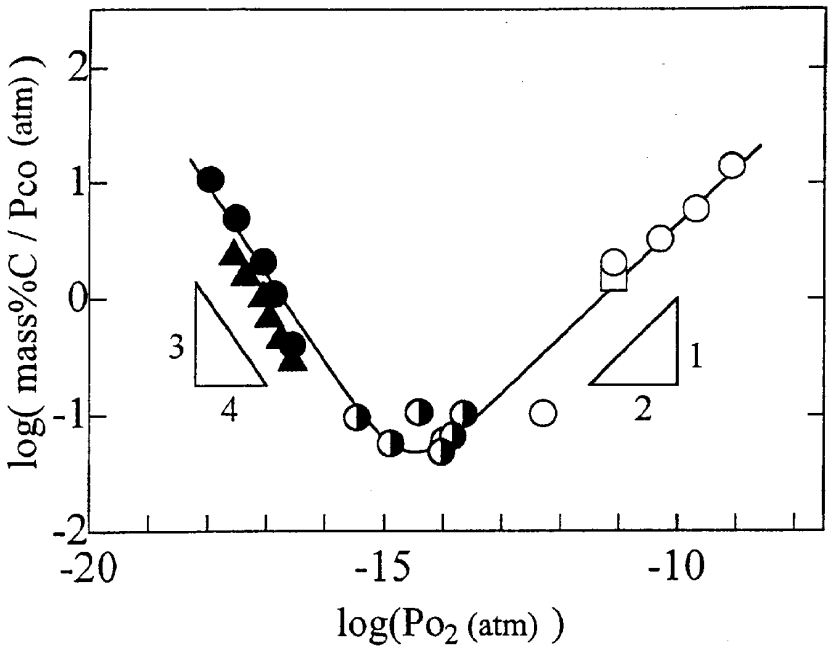

Fig. 17. Relationship between log(P_{O2}) and log(mass%C/P_{CO}) for 80mass%BaO-MnO slags at 1573K.

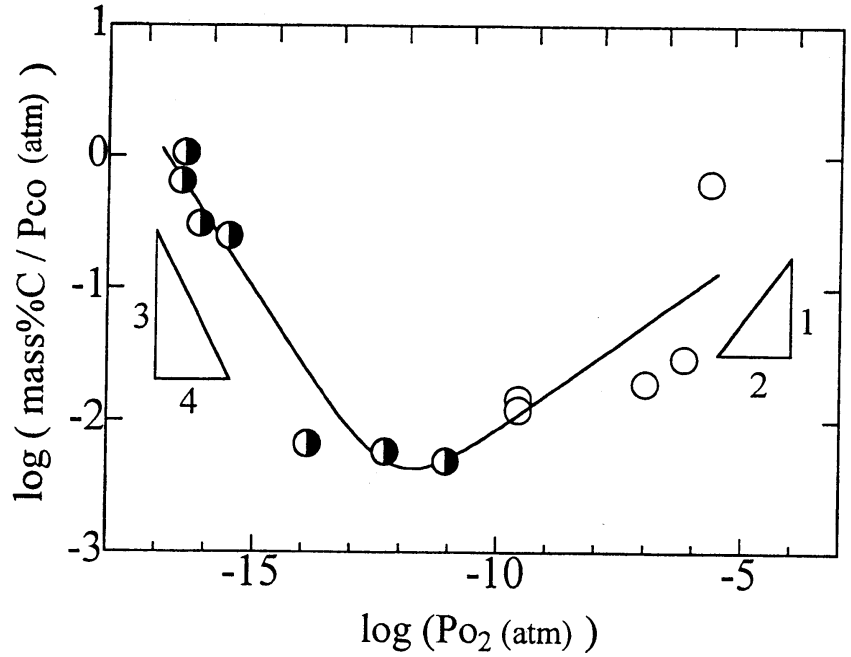

Fig. 18. Relationship between log(P_{O2}) and log(mass%C/P_{CO}) for $CaO_{satd.}$-B_2O_3 slags at 1733K.

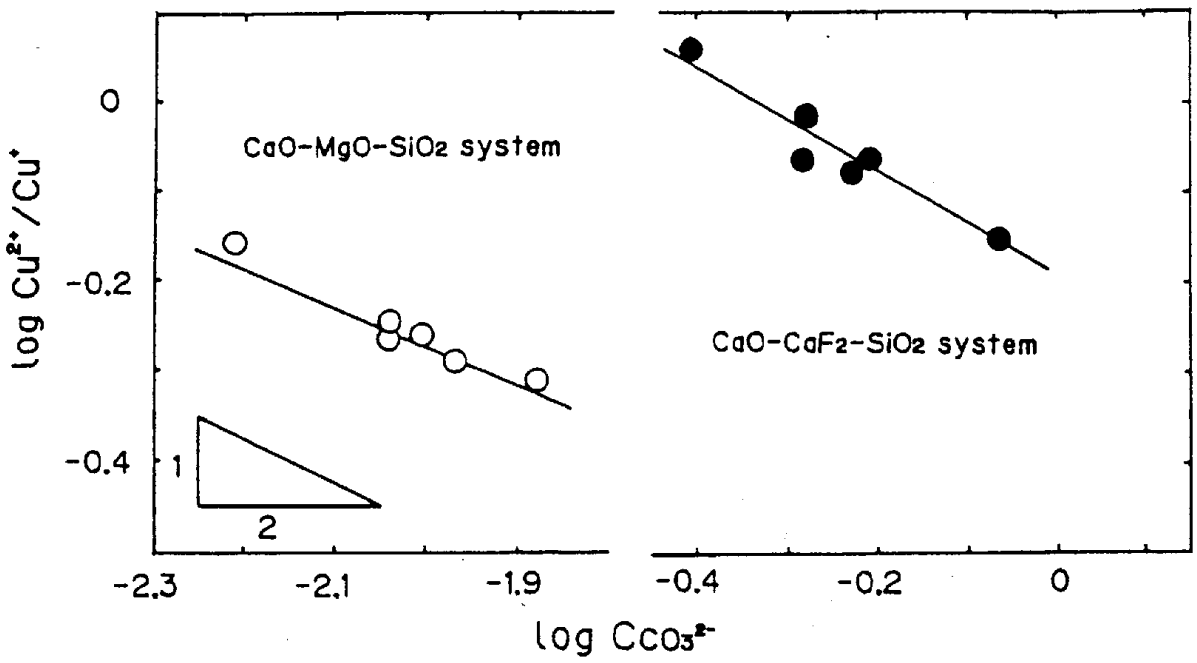

Fig. 19. Relationship between the Cu^{2+}/Cu^{+} ratio and carbonate capacity for the CaO-33mol%CaF_2-SiO_2 and CaO-MgO-43mol%SiO_2 systems at 1573 and 1773K, respectively.

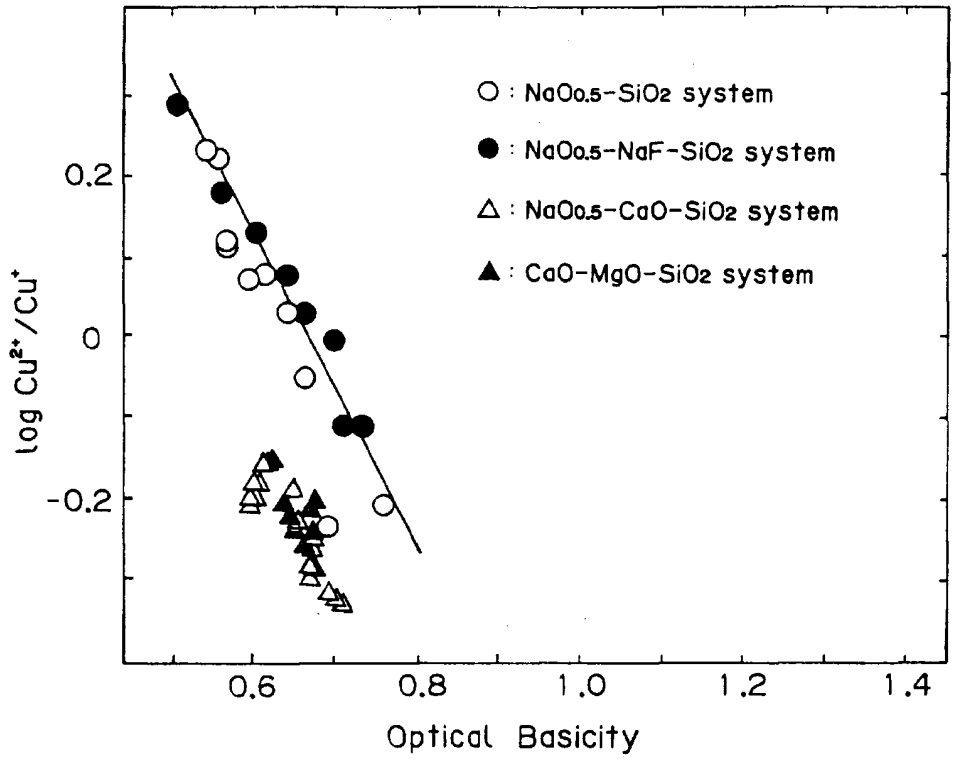

Fig. 20. Relationship between the Cu^{2+}/Cu^{+} ratio and optical basicity for the $NaO_{0.5}$-SiO_2 (Cu^{2+}/Cu^{+} at 1373K), $NaO_{0.5}$-NaF-SiO_2 (Cu^{2+}/Cu^{+} at 1373K), $NaO_{0.5}$-CaO-SiO_2 (Cu^{2+}/Cu^{+} at 1673K), and CaO-MgO-SiO_2 (Cu^{2+}/Cu^{+} at 1773K) systems. The basicity value of NaF is assumed to be zero.

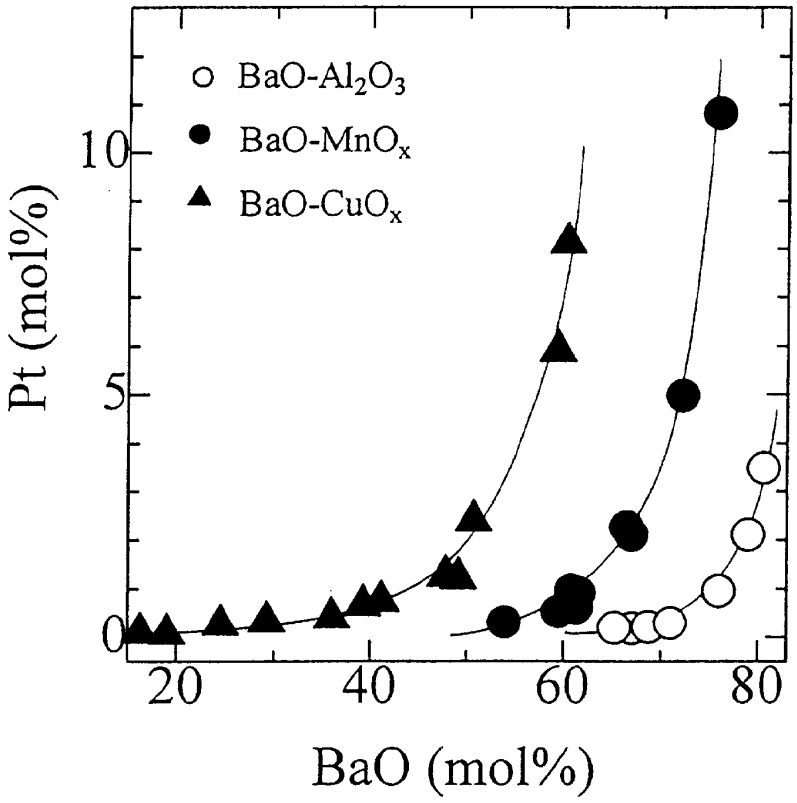

Fig. 21. Dependence of Pt solubility on content of BaO for the $BaO\text{-}Al_2O_3$, $BaO\text{-}MnO_x$, and $BaO\text{-}CuO_x$ melts at 1873K.

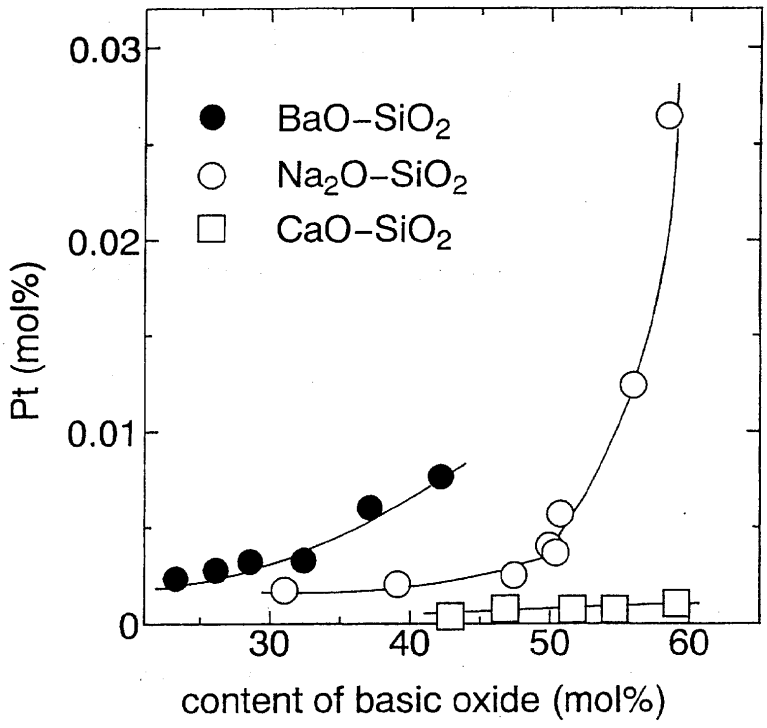

Fig. 22. Dependence of Pt solubility on content of basic oxide for the $BaO\text{-}SiO_2$, $Na_2O\text{-}SiO_2$, and $CaO\text{-}SiO_2$ systems in air at 1873K.

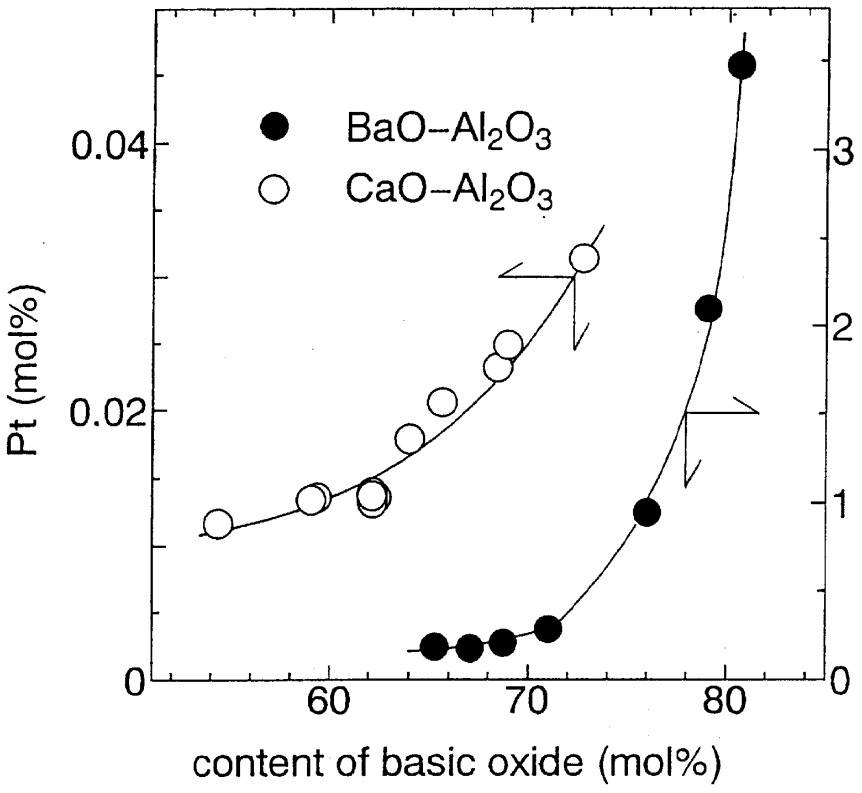

Fig. 23. Dependence of Pt solubility on content of basic oxide for the $BaO\text{-}Al_2O_3$, and $CaO\text{-}Al_2O_3$ systems in air at 1873K.

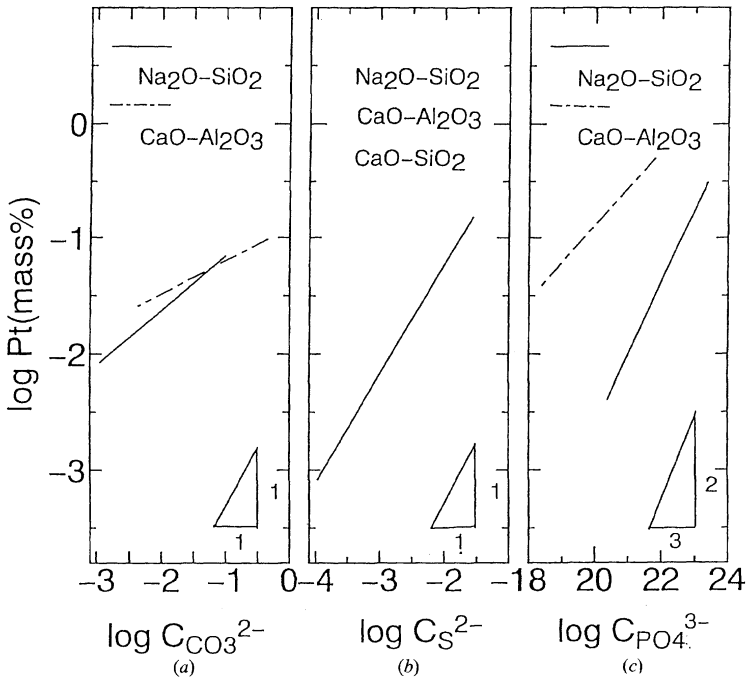

Fig. 24. Relationship between (a) carbonate, (b) sulfide, and (c) phosphate capacities and Pt solubility.

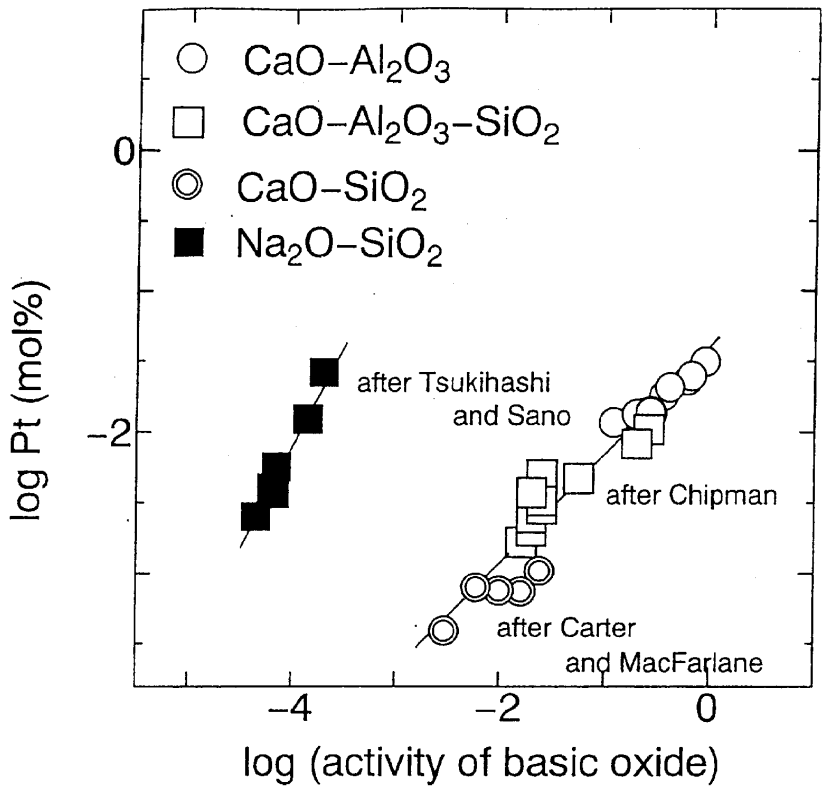

Fig. 25. Dependence of Pt solubility on the activity of basic oxide.

Fig. 26. Relationship between theoretical optical basicity and Pt solubility.